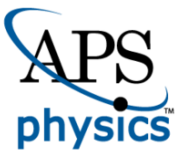

Dephasingless Laser Wakefield Acceleration

J. P. Palastro, J. L. Shaw, P. Franke, D. Ramsey, T. T. Simpson, and D. H. Froula

Phys. Rev. Lett. **124**, 134802 — Published 31 March 2020

DOI: 10.1103/PhysRevLett.124.134802

Dephasingless Laser Wakefield Acceleration

J.P. Palastro, J.L. Shaw, P. Franke, D. Ramsey, T.T. Simpson, and D.H. Froula
University of Rochester, Laboratory for Laser Energetics, Rochester, New York 14623, USA

Abstract

Laser wakefield accelerators (LWFAs) produce extremely high gradients enabling compact accelerators and radiation sources, but face design limitations, such as dephasing, occurring when trapped electrons outrun the accelerating phase of the wakefield. Here we combine spherical aberration with a novel cylindrically symmetric echelon optic to spatiotemporally structure an ultra-short, high-intensity laser pulse that can overcome dephasing by propagating at any velocity over any distance. The ponderomotive force of the spatiotemporally shaped pulse can drive a wakefield with a phase velocity equal to the speed of light in vacuum, preventing trapped electrons from outrunning the wake. Simulations in the linear regime and scaling laws in the bubble regime illustrate that this dephasingless LWFA can accelerate electrons to high energies in much shorter distances than a traditional LWFA—a single 4.5 m stage can accelerate electrons to TeV energies without the need for guiding structures.

Forty years ago, Tajima and Dawson recognized that the axial electric fields of ponderomotively driven plasma waves far surpass those of conventional radiofrequency accelerators [1], launching the field of 'advanced accelerators'—disruptive concepts that promise smaller-scale, cheaper accelerators for high energy physics experiments and advanced light sources [2,3]. Since their seminal paper, a number of theoretical breakthroughs [4-7] and experimental demonstrations [8-14] of laser wakefield acceleration (LWFA) have made rapid progress toward that goal. Experiments recurrently achieve record-breaking electron energy gains underscored by the recent observation of a 7.8 GeV energy gain in only 20 cm [15]. In spite of this impressive progress, traditional LWFA faces a key design limitation of electrons outrunning the accelerating phase of the wakefield or dephasing.

In traditional LWFA, a near-collimated laser pulse, either through channel or self-guiding, produces a ponderomotive force that travels subluminally at the group velocity (

$v_g < c$). The phase velocity of the resulting wakefield equals the velocity of the ponderomotive force. As a result, high-energy electrons, travelling at near the vacuum speed of light ($v_e \simeq c$), escape the accelerating phase of wakefield after a dephasing length, $L_d \propto n_0^{-3/2}$, where n_0 is the plasma density. Because the maximum accelerating field scales as $E_{\max} \propto n_0^{1/2}$, a lower plasma density will increase the maximum energy gain of electrons, $\Delta\gamma \propto n_0^{-1}$, but will greatly increase the length of the accelerator [2]. As an example, a single-stage 1-TeV accelerator would require at least 200 m of uniform, low-density plasma, the creation of which would represent a technical feat unto itself. Even if this accelerator could be realized, the low plasma density would lead to a higher bunch charge, $N \sim n_0^{-1/2}$, which would enhance beamstrahlung, potentially limiting its efficacy as an electron-positron collider [16]. Instead, the current paradigm within the LWFA community envisions a TeV LWFA composed of multiple ~10 GeV stages, which could be optimized for efficiency, by matching the dephasing length to the depletion length of the laser pulse, and designed to balance tradeoffs between signal and beamstrahlung [16]. This approach, however, comes with its own set of challenges, such as precisely timing the injection of the electron beam and laser pulses into each of the stages.

Spatiotemporal shaping of laser pulses provides control over the velocity of an intensity peak or ponderomotive force [17-19]. By stretching the region over which a laser pulse focuses and adjusting the relative timing at which those foci occur, the velocity of an intensity peak can be made to travel at any velocity, independent of the group velocity. This property has already been exploited in proof-of-principle simulations to improve Raman amplification, photon acceleration, and relativistic mirrors, and to generate Cherenkov radiation in a plasma [17-23] and in experiments to drive ionization waves at any velocity [24]. For LWFA, a spatiotemporally shaped laser pulse could drive a wakefield with a phase velocity equal to the speed of light in vacuum ($v_p = c$), eliminating dephasing and greatly reducing the accelerator length by allowing for operation at higher densities. In addition, the stretched focal region eliminates the need for an external guiding structure or self-guiding. This was previously proposed using chromatic focusing of chirped laser pulses, but the technique inherently generated long

pulses, diminishing its utility for LWFA [19]. Furthermore, the maximum extent of the focal region was limited to a single dephasing length.

In this Letter, we describe a dephasingless wakefield accelerator (DLWFA) enabled by a novel optical technique for spatiotemporal pulse shaping that provides control over the phase velocity of the wakefield while preserving the ultrashort duration of the ponderomotive force. In the nonlinear regime ($a_0 > 1$, where $a_0 = eA/m_e c$ is the normalized vector potential of the laser) a DLWFA can achieve TeV energy gains in only 4.5 m—40 times shorter than traditional LWFA. Simulations in the linear regime ($a_0 < 1$) demonstrate a 1.3 GeV energy gain in *~3.5 times less distance* than a traditional LWFA (8 cm vs 28 cm). The optical technique combines the recently described axiparabola [25] with a novel echelon optic. The axiparabola creates an extended focal region, eliminating the need for guiding, while the echelon adjusts the temporal delay to provide the desired ponderomotive velocity. This concept improves upon the chromatic flying focus [19] by providing the original features of a small focal spot that can propagate at any velocity over any distance, while using an achromatic focusing system to maintain a transform-limited pulse duration ideal for LWFA. The concept does not require (1) the plasma to be colocated with an active lasing media [26], (2) a structured plasma [27], or (3) multiple intersecting laser pulses [28]. In contrast to the pair of laser pulses with tilted pulse fronts employed in the traveling wave electron acceleration described by Debus *et al.* [28], the axiparabola-echelon pair delivers a single laser pulse that can drive a cylindrically symmetric wakefield, preserving the favorable focusing fields and maintaining the strong electrostatic fields resulting from near spherical expulsion of electrons in the bubble regime. Further, by adjusting the profile of the echelon, the ponderomotive force can be made to follow a dynamic trajectory, with either accelerations or decelerations to control trapping and reduce dark current.

Figure 1(a) highlights the advantage of the DLWFA in the linear regime by comparing the energy gains as a function of accelerator length for a DLWFA, a traditional LWFA, and a conventional radiofrequency accelerator. The advantage of the DLWFA increases with the energy gain or accelerator length, i.e. the DLWFA achieves the same energy as a traditional LWFA with an increasingly smaller distance. Scaling

laws in the linear regime illustrate this behavior. The energy gain of a DLWFA scales as $W_D = (\pi/8)(k_{pl}L)a_0^2$, where L is the accelerator length, $k_{pl} = \pi/c\tau_l$, τ_l is the transform-limited pulse duration of the laser, and energies are normalized by $m_e c^2$ throughout. Maximizing the energy gain requires operating at the highest possible density, $n_{\max} = \pi^2 \varepsilon_0 m_e / e^2 \tau_l^2$, and increasing the length of the plasma as much as possible. This is in contrast to the scaling of a traditional LWFA, which requires operating at lower densities to increase the dephasing length, and hence the energy gain: $W_T = (\pi/8)(k_p L_d)a_0^2$ where $L_d = 2\pi k_0^2 / k_p^3$ is the dephasing length, $k_0 = 2\pi/\lambda_0$ is the central wavenumber of the laser, λ_0 the wavelength, and $k_p = (e^2 n_0 / m_e c^2 \varepsilon_0)^{1/2}$ [2]. From the two scaling laws, the traditional LWFA only attains a fraction of the DLWFA gain over the same distance, $W_T = (\omega_0 \tau_l / \pi)^{2/3}(2c\tau_l / L)^{1/3} W_D$, or must have a length $L_d = (\pi/\omega_0\tau_l)(L/2c\tau_l)^{1/2} L$ to attain the same energy gain.

A dephasingless wakefield can be excited by a pondermotive force that travels through the plasma at the speed of light in vacuum over a distance greater than the dephasing length. The novel spatiotemporal technique employed here and depicted in Fig. 2 accomplishes this using two optics: an axiparabola [25] and a cylindrically symmetric echelon. The axiparabola creates an extended focal region by focusing different radial locations in the near field to different axial locations in the far field. The echelon adjusts the temporal delay of radial locations in the near field to produce the desired ponderomotive or "focal" velocity. The combined axiparabola-echelon system delivers an ultrashort pulse to each axial location in the focal region without unwanted focusing aberrations and a duration equal to that of the incident pulse.

Simulations, which implement the optical configuration shown in Fig. 2 and evolve test electrons in the resulting wakefield, reproduce the analytic scaling for the energy gain shown in Fig. 1(a) (dots). To overcome the subluminal group velocity, $v_g / c \simeq 1 - \omega_p^2 / 2\omega_0^2$, and ensure a focal velocity $v_f = c$ in the plasma, the echelon was tuned to produce a vacuum focal velocity $v_f / c = 1 + \omega_p^2 / 2\omega_0^2$. For the parameters considered, the finite spot size correction to the group velocity can be neglected: $\Delta v_g = -1/16 f_\#^2 \approx -1 \times 10^{-3}$ where $f_\#$ is the f-number of the axiparabola. The distinct plasma dispersion experienced by each ring of the pulse on its way to focus was

compensated with a radially varying linear chirp. In practice, this modest chirp could be implemented using chirped coatings on the echelon. The simulations solved the modified-paraxial wave equation [29] and used the Green's function approach to calculate the longitudinal and transverse wakefields at each point in the focal region [2]. Test electrons were integrated in the calculated wakefields. The dots correspond to the maximum energy gain of test electrons injected with an initial energy of $\gamma_0 = 60$.

Figure 3(a) shows that the on-axis laser intensity and phase fronts of the axial wakfield propagate over an extended distance, $L = 8$ cm, at the speed of light in vacuum—contours of constant $\xi = t - z/c$. To compare with a traditional LWFA, Fig. 3(b) displays the on-axis intensity and axial wakefield resulting from an axiparabola-echelon pair configured for a focal velocity equal to the group velocity in the plasma, $v_f = v_g \simeq c(1-\omega_p^2/2\omega_0^2)$. Note that the extended focal region provided by the axiparabola serves as a surrogate for channel guiding. Both the intensity peaks and phase fronts slip backwards in the moving frame consistent with $v_g < c$. Figure 4 shows the energy gain of optimal test electrons evolved in the wakefields shown in Fig. 3. In a traditional LWFA the electron outruns the laser pulse and only gains energy over a single dephasing length, reaching a maximum energy of $\gamma_f = 75$ MeV compared to $\gamma_f = 1.3$ GeV for the DLWFA. In the simulations, the plasma density was uniform. To ensure that axial density gradients do not reintroduce dephasing, the variation in density should satisfy $\delta\omega_p^2 < 2\pi\omega_0^2 / k_p L$.

The advantages of DLWFA do not come without a tradeoff: a laser pulse must be more energetic to drive a dephasingless wakefield with the same final energy gain as a traditional LWFA. Because the axiparabola distributes the energy density of the pulse over a length L, the pulse must contain L/z_R more energy for the same peak intensity (or a_0) as a pulse focused by an achromatic lens, where z_R is the Rayleigh range of the achromat focal spot. As a result, the ratio of pulse energies needed for DLWFA and traditional LWFA is given by $U_D / U_T = 2(2/\pi)^4(\omega_0\tau_l)^2(2c\tau_l/L)^{1/2}$, where the spot size for the traditional LWFA was set to $w_T = \pi / k_p$ (larger spot sizes make the scaling more favorable for DLWFA). As an example, a 10 GeV energy gain for the parameters used in Fig. 1 requires one tenth the distance but $U_D \sim 6U_T$. While it may appear that the higher

energy would make DLWFA susceptible to nonlinear effects such as self-focusing and spectral broadening, the energy of the structured pulse is essentially spread out over L, such that the local power is moderate. Furthermore, each radial segment of the pulse comes in and out of focus within the Rayleigh range associated with the f-number of the axiparabola, and thus only exhibits a high intensity over a very short distance. Furthermore, the efficiency of laser energy into electrons, $\eta = NW/U$, for DLWFA will generally be less for the same final energy gain. For the current example $U_D L_d \approx 2U_T L$, providing $\eta_D \sim 2(A_D/A_T)\eta_T$, where A is the cross sectional area of the accelerated beams. Using $w_T = \pi/k_p$, $\eta_D \sim 32 f_\#^2 (\lambda_0/L_d)^{2/3}\eta_T \sim .05$.

The design of the axiparabola starts with (1) the notion that rings in the near field can be focused to different locations in the far field (similar to an axicon) and (2) the condition that the focused intensity of each of these rings is equal [25]. Using ray-optics one can show that the effective focal length $f = f_0 + (r/R)^2 L$ satisfies this condition, where f_0 is the focal length of a near-center ray, r is the radial coordinate in the near field, and R is the aperture radius. The focal length, in turn, defines the shape of the optic or sag function, $z(r)$, and the phase to apply to the frequency domain laser field in the simulations, $\phi(r) = -2\omega z(r)/c$. While the phase includes higher order spatial "aberrations," the axiparabola essentially adds spherical aberration to increase the focal range: $\phi \approx -(kr^2/2f_0)[1-(Lr^2/2f_0R^2)]$.

The velocity of the focus, v_f, is determined by the distance and time of flight for each ray from a point on the optic to its focus, $f(r)$. For a desired focal velocity, a radially dependent delay can be applied across the pulse, $\delta(r)$. Using ray-optics, one can show that a delay

$$\delta_r = \left[\frac{c}{v_f} - \left(\frac{1-z_r^2}{1+z_r^2}\right)\right]\frac{2Lr}{cR^2} \quad (1)$$

could provide the desired focal velocity, where the subscript denotes differentiation with respect to r. To maintain a transform limited pulse duration and avoid the complications of a continuous phase, a reflective echelon is employed. The echelon effectively multiplexes different rings into separate pulses. By ensuring that the steps of the echelon are integer wavelengths deep, the phase fronts of the pulse will remain coherent, but the

desired "group delay" will be imparted. Given $\delta(r)$, the simplest implementation of the echelon can be created as follows: $\delta_{\text{ech}} = \frac{1}{4}\lambda_0[\text{ceil}(\delta/\lambda_0) + \text{floor}(\delta/\lambda_0)]$. The additional factor of one half (other than the averaging) accounts for the fact that the incoming light travels past the outermost reflection point twice, once as it is incident and again after it is reflected. The axiparabola (minus the parabolic phase) and the echelon used for the simulations are shown in Fig. 5. While the depth of each echelon step is one half wavelength, the radial width of each echelon tier is much larger than a wavelength. As a result, the echelon acts essentially like a mirror with almost no diffractive losses.

In principle, the axiparabola-echelon pair could be designed to deliver an accelerating intensity peak to control trapping and reduce dark current [30], providing low energy-spread electron bunches. Following a similar analysis as presented in Refs. [27,30], the linear regime DLWFA will trap electrons with an initial axial momentum greater than the threshold $p_{th} = c^{-1}v_f\gamma_f(1+\gamma_f E_{\max}) - \gamma_f[(1+\gamma_f E_{\max})^2 - 1]^{1/2}$ where $\gamma_f = (1 - v_f^2/c^2)^{-1/2}$ and $E_{\max} \sim \pi a_0^2/8$. Starting the focal velocity at $v_f = 0.9c$ allows the wakefield to trap a desired number of slow electrons, $\gamma_0 \sim 1.5$. Subsequently accelerating the focal velocity from $v_f = 0.9c$ to $v_f = c$ would terminate additional trapping by raising the threshold to its asymptotic value $p_{th} \sim 1 + 2/\pi a_0^2$.

The promise of extending DLWFA to the nonlinear bubble regime—a TeV accelerator in 4.5 m—is illustrated by Fig. 1(b). For a nonlinear DLWFA, $W_D = \frac{1}{2}(k_{pl}L)a_0^{1/2}$, where now $k_{pl} \sim a_0^{1/2}/c\tau_l$ in order to match (roughly) half the bubble radius to the transform-limited pulse duration. As before, operating at the highest possible density and increasing the plasma length maximizes the energy gain. The traditional LWFA must have a length $L_d = (3a_0/4)^{1/2}(\omega_0\tau_l)^{-1}(L/c\tau_l)^{1/2}L$ to match the energy gain of a DLWFA, and only reaches a fraction of the DLWFA gain over the same distance, $W_T = (4/3a_0)^{1/3}(\omega_0\tau_l)^{2/3}(c\tau_l/L)^{1/3}W_D$, where $W_T = \frac{1}{2}(k_p L_d)a_0^{1/2}$ and $L_d = (4/3)a_0^{1/2}k_0^2/k_p^3$ [6]. The promise of these scalings warrants future, full format particle-in-cell simulations to verify their predictions.

A novel electron acceleration concept based on the recently demonstrated "flying focus" technology offers a new paradigm for LWFA [18]. A combined axiparabola-echelon optic was used to spatiotemporally structure a laser pulse with an ultrashort

(transform limited) intensity peak that travels through meters of plasma at the speed of light in vacuum while maintaining a small focal spot and high-intensity. In this dephasingless laser wakefield accelerator, the plasma density, and therefore the accelerating gradient, is decoupled from the speed of the intensity peak. By leveraging the horizon laser systems in development throughout the world, DLWFA can enable two critical experimental platforms: First, a kHz repetition rate laser system that delivers 30 fs, 3J laser pulses could drive DLWFA in the linear regime, delivering ~2 GeV electron beams and the associated radiation sources every millisecond. Second, scaling laws for DLWFA in the nonlinear regime suggest that a 15 fs, 500 J laser could accelerate electrons to a 100 GeV in a single half-meter stage—a 20 times shorter distance than a traditional LWFA. Unlike traditional LWFA, where higher electron energy gains require longer laser pulses to match the plasma wavelength and increased laser energy to maintain high intensities, DLWFA is ideally suited for these high energy ultrashort pulses. These single-stage plasma accelerators could provide the compact particle and radiation sources needed (1) to probe high energy-density matter with unprecedented detail and repetition rate and (2) to access new frontiers of nonperturbative, collective strong field QED.

Acknowledgements

The authors would like to thank D. Turnbull, R.K. Follett, C. Dorrer, and J. Bromage for fruitful discussions.

The work published here was supported by the US Department of Energy Office of Fusion Energy Sciences under contract no. DE-SC0016253, the Department of Energy under cooperative agreement no. DE-NA0003856, the University of Rochester, and the New York State Energy Research and Development Authority.

This report was prepared as an account of work sponsored by an agency of the U.S. Government. Neither the U.S. Government nor any agency thereof, nor any of their employees, makes any warranty, express or implied, or assumes any legal liability or responsibility for the accuracy, completeness, or usefulness of any information, apparatus, product, or process disclosed, or represents that its use would not infringe

privately owned rights. Reference herein to any specific commercial product, process, or service by trade name, trademark, manufacturer, or otherwise does not necessarily constitute or imply its endorsement, recommendation, or favoring by the U.S. Government or any agency thereof.

References

[1] T. Tajima and J.M. Dawson, "Laser Electron Accelerator," Phys. Rev. Lett. **43**, 267 (1979).

[2] E. Esarey, C.B. Schroeder, and W.P. Leemans, "Physics of laser-driven plasma-based electron accelerators," Reviews of Modern Physics **81**, 1229 (2009).

[3] F. Albert, A.G.R. Thomas, S.P.D. Mangles, S. Banerjee, S. Corde, A. Flacco, M. Litos, D. Neely, J. Vieira, Z. Najmudin *et al.*, "Laser wakefield accelerator based light sources: potential applications and requirements," Plasma Physics and Controlled Fusion **56**, 084015 (2014).

[4] P. Sprangle, E. Esarey, A. Ting, and G. Joyce, "Laser Wakefield Acceleration and Relativistic Optical Guiding," Appl. Phys. Lett. **53**, 2146 (1988).

[5] S. Gordienko and A. Pukhov, "Scalings for ultrarelativistic laser plasmas and quasimonoenergetic electrons," Physics of Plasmas **12**, 043109 (2005).

[6] W. Lu, M. Tzoufras, C. Joshi, F.S. Tsung, W.B. Mori, J. Vieira, R.A. Fonseca, and L.O. Silva, "Generating Multi-GeV Electron Bunches Using Single Stage Laser Wakefield Acceleration in a 3D Nonlinear Regime," Phys. Rev. ST Accel. Beams **10**, 061301 (2007).

[7] J.L. Vay, "Noninvariance of Space- and Time-Scale Ranges under a Lorentz Transformation and the Implications for the Study of Relativistic Interactions," Physical Review Letters **98**, 130405 (2007).

[8] J. Faure, Y. Glinec, A. Pukhov, S. Kiselev, S. Gordienko, E. Lefebvre, J.-P. Rousseau, F. Burgy, and V. Malka, "A Laser-Plasma Accelerator Producing Monoenergetic Electron Beams," Nature **431**, 541 (2004).

[9] C.G.R. Geddes, C. Toth, J. van Tilborg, E. Esarey, C.B. Schroeder, D. Bruhwiler, C. Nieter, J. Cary, and W.P. Leemans, "High-Quality Electron Beams from a Laser Wakefield Accelerator Using Plasma-Channel Guiding," Nature **431**, 538 (2004).

[10] S.P.D. Mangles, C.D. Murphy, Z. Najmudin, A.G.R. Thomas, J.L. Collier, A.E. Dangor, E.J. Divall, P.S. Foster, J.G. Gallacher, C.J. Hooker *et al.*, "Monoenergetic Beams of Relativistic Electrons from Intense Laser–Plasma Interactions," Nature **431**, 535 (2004).

[11] B.B. Pollock, C.E. Clayton, J.E. Ralph, F. Albret, A. Davidson, L. Divol, C. Filip, S.H. Glenzer, K. Herpoldt, W. Lu *et al.*, "Demonstration of a Narrow Energy Spread, ~0.5 GeV Electron Beam from a Two-Stage Laser Wakefield Accelerator," Phys. Rev. Lett. **107**, 045001 (2011).

[12] X. Wang, R. Zgadzaj, N. Fazel, Z. Li, S.A. Yi, X. Zhang, W. Henderson, Y.Y. Chang, R. Korzekwa, H.E. Tsai *et al.*, "Quasi-monoenergetic laser-plasma acceleration of electrons to 2□GeV," Nature Communications **4**, 1988 (2013).

[13] H.T. Kim, K.H. Pae, H.J. Cha, I.J. Kim, T.J. Yu, J.H. Sung, S.K. Lee, T.M. Jeong, and J. Lee, "Enhancement of Electron Energy to the Multi-GeV Regime by a Dual-Stage Laser-Wakefield Accelerator Pumped by Petawatt Laser Pulses," Phys. Rev. Lett. **111**, 165002 (2013).
[14] S. Steinke, J. van Tilborg, C. Benedetti, C.G.R. Geddes, C.B. Schroeder, J. Daniels, K.K. Swanson, A.J. Gonsalves, K. Nakamura, N.H. Matlis *et al.*, "Multistage coupling of independent laser-plasma accelerators," Nature **530**, 190 (2016).
[15] A.J. Gonsalves, K. Nakamura, J. Daniels, C. Benedetti, C. Pieronek, T.C.H. de Raadt, S. Steinke, J.H. Bin, S.S. Bulanov, J. van Tilborg *et al.*, "Petawatt Laser Guiding and Electron Beam Acceleration to 8 GeV in a Laser-Heated Capillary Discharge Waveguide," Physical Review Letters **122**, 084801 (2019).
[16] C.B. Schroeder, E. Esarey, C.G.R. Geddes, C. Benedetti, and W.P. Leemans, "Physics Considerations for Laser-Plasma Linear Colliders," Phys. Rev. ST Accel. Beams **13**, 101301 (2010).
[17] A. Sainte-Marie, O. Gobert, and F. Quéré, "Controlling the Velocity of Ultrashort Light Pulses in Vacuum Through Spatio-Temporal Couplings," Optica **4**, 1298 (2017).
[18] D.H. Froula, D. Turnbull, A.S. Davies, T.J. Kessler, D. Haberberger, J.P. Palastro, S.-W. Bahk, I.A. Begishev, R. Boni, S. Bucht *et al.*, "Spatiotemporal Control of Laser Intensity," Nat. Photonics **12**, 262 (2018).
[19] D.H. Froula, J.P. Palastro, D. Turnbull, A. Davies, L. Nguyen, A. Howard, D. Ramsey, P. Franke, S.W. Bahk, I.A. Begishev *et al.*, "Flying focus: Spatial and temporal control of intensity for laser-based applications," Physics of Plasmas **26**, 032109 (2019).
[20] D. Turnbull, S. Bucht, A. Davies, D. Haberberger, T. Kessler, J.L. Shaw, and D.H. Froula, "Raman Amplification with a Flying Focus," Phys. Rev. Lett. **120**, 024801 (2018).
[21] A.J. Howard, D. Turnbull, A.S. Davies, P. Franke, D.H. Froula, and J.P. Palastro, "Photon Acceleration in a Flying Focus," Physical Review Letters **123**, 124801 (2019).
[22] P. Franke, J.P. Palastro, D. Turnbull, and D.H. Froula, "Frequency Conversion and Intensification of Laser Pulses Reflected from Ionization Waves of Arbitrary Velocity," Bull. Am. Phys. Soc., T07.00008 (2019).
[23] J. Palastro, T.M. Antonsen, A. Colaïtis, R. Follett, D. Turnbull, J.M. Vieira, and D.H. Froula, "Cherenkov Radiation from a Plasma," Bull. Am. Phys. Soc., JO8.00008 (2018).
[24] D. Turnbull, P. Franke, J. Katz, J.P. Palastro, I.A. Begishev, R. Boni, J. Bromage, A.L. Milder, J.L. Shaw, and D.H. Froula, "Ionization Waves of Arbitrary Velocity," Phys. Rev. Lett. **120**, 225001 (2018).
[25] S. Smartsev, C. Caizergues, K. Oubrerie, J. Gautier, J.-P. Goddet, A. Tafzi, K.T. Phuoc, V. Malka, and C. Thaury, "Axiparabola: a long-focal-depth, high-resolution mirror for broadband high-intensity lasers," Optics Letters **44**, 3414 (2019).
[26] D.L. Fisher and T. Tajima, "Superluminous laser pulse in an active medium," Physical Review Letters **71**, 4338 (1993).

[27] S.J. Yoon, J.P. Palastro, and H.M. Milchberg, "Quasi-Phase-Matched Laser Wakefield Acceleration," Phys. Rev. Lett. **112**, 134803 (2014).
[28] A. Debus, R. Pausch, A. Huebl, K. Steiniger, R. Widera, T.E. Cowan, U. Schramm, and M. Bussmann, "Circumventing the Dephasing and Depletion Limits of Laser-Wakefield Acceleration," Physical Review X **9**, 031044 (2019).
[29] J.P. Palastro, D. Turnbull, S.-W. Bahk, R.K. Follett, J.L. Shaw, D. Haberberger, J. Bromage, and D.H. Froula, "Ionization Waves of Arbitrary Velocity Driven by a Flying Focus," Phys. Rev. A **97**, 033835 (2018).
[30] C.B. Schroeder, E. Esarey, B.A. Shadwick, and W.P. Leemans, "Trapping, dark current, and wave breaking in nonlinear plasma waves," Physics of Plasmas **13**, 033103 (2006).

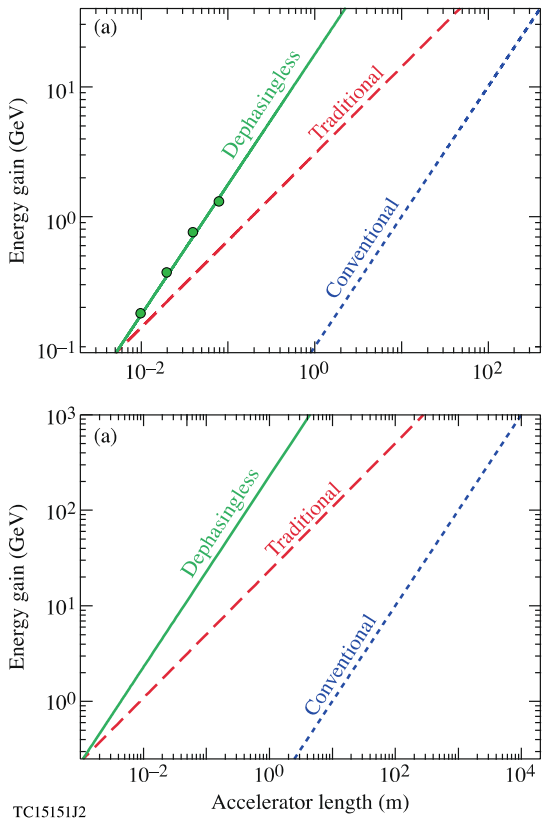

Figure 1. Energy gain of a DLWFA and traditional LWFA in the (a) linear ($a_0 = 0.5$) and (b) nonlinear ($a_0 = 4$) regimes as function of accelerator length compared with a conventional radio-frequency accelerator. The linear regime DLWFA achieves an energy gain of 10 GeV in 10 times less distance than a traditional LWFA. Simulations (dots) show excellent agreement with the theoretical scaling. The nonlinear DLWFA reaches a TeV energy gain in 4.5 m, 40 times less distance than a traditional LWFA. The energy gain for the conventional accelerator is determined by the electric field threshold for material damage, $W_C = E_{thr} L$ where $E_{thr} = 100$ MeV / m. The linear and nonlinear wakefields were driven by a 1 μm laser with $\tau_l = 30$ fs and $\tau_l = 15$ fs, respectively.

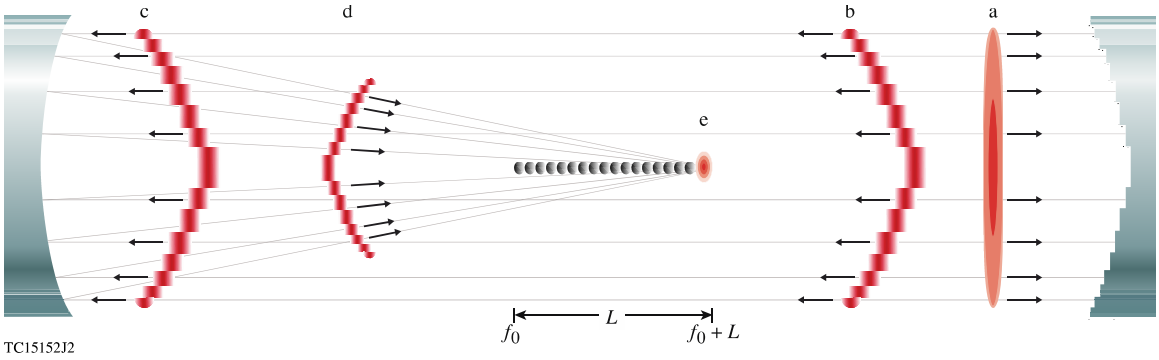

Figure 2. A schematic of the optical configuration enabling the DLWFA. (a-b) The laser pulse first reflects off of a stepped echelon, which imparts the temporal delay required for a focal velocity equal to the speed of light in vacuum without introducing angular dispersion or aberrated focusing. (c-d) After reflecting from the echelon, the pulse encounters the axiparabola, which focuses different rings in the near field to different axial locations in the far-field, stretching the region over which the pulse can sustain a high intensity from the initial focus at f_0 to $f_0 + L$. (e) The pulse drives a wakefield at the speed of light in vacuum.

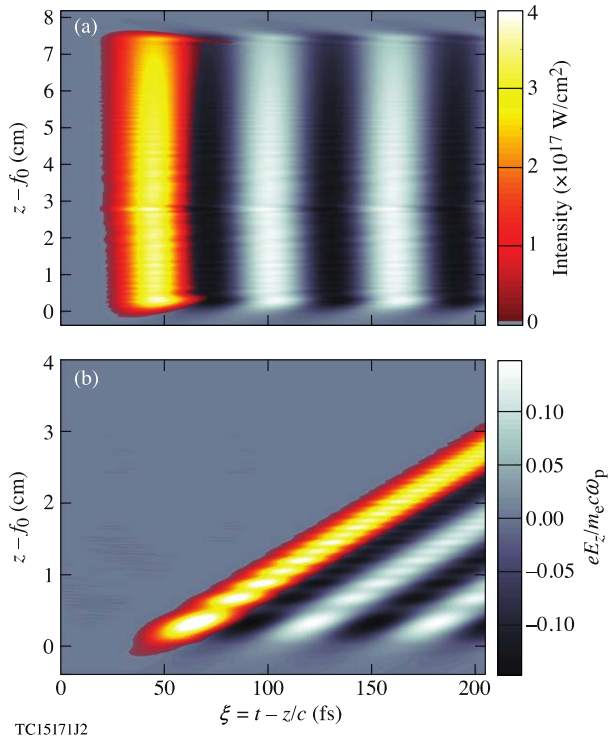

Figure 3. (a) The on-axis intensity of a pulse spatiotemporally structured by an axiparabola-echelon pair with $v_f = c$, $f_\# = f_0 / 2R = 7$ and $L = 8$ cm, orange scale, and the resulting on-axis axial wakefield, grey scale, as a function of propagation distance $z - f_0$ and speed of light frame coordinate, $\xi = t - z/c$. The peak intensity of the laser pulse and the phase fronts of the wakefield travel at the speed of light in vacuum ($\xi = \text{const.}$). (b) The same quantities for an axiparabola-echelon pair with $v_f = v_g$, which emulates a traditional LWFA with guiding. On account of their subluminal velocity, the peak intensity of the laser pulse and the phase fronts slip backwards in the speed of light frame, $\xi \approx (\omega_p^2 / 2c\omega_0^2)z$.

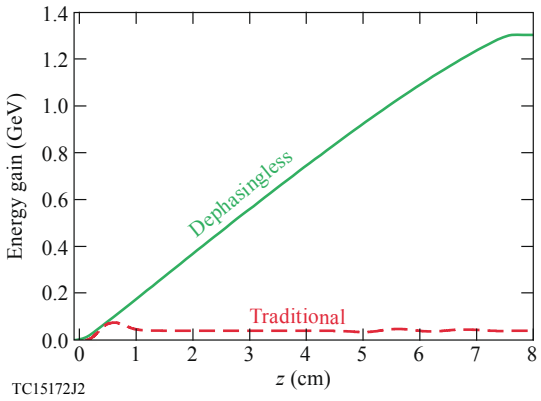

Figure 4. Comparison of the maximum energy gain of electrons simulated in a DLWFA with $L = 8$ cm and in a traditional LWFA emulated by a spatiotemporally structured pulse with $v_f = v_g$. For both the DLWFA and traditional LWFA, $\lambda_0 = 1$ μm, $\tau_l = 30$ fs, $a_0 = 0.5$, and, $n_0 = 3.5 \times 10^{18}$ cm^{-3}. In the DLWFA, the electron gains energy 1.3 GeV over 16 dephasing lengths, while in the traditional LWFA, the electron outruns the laser pulse and only gains a maximum of 75 MeV energy over a single dephasing length.

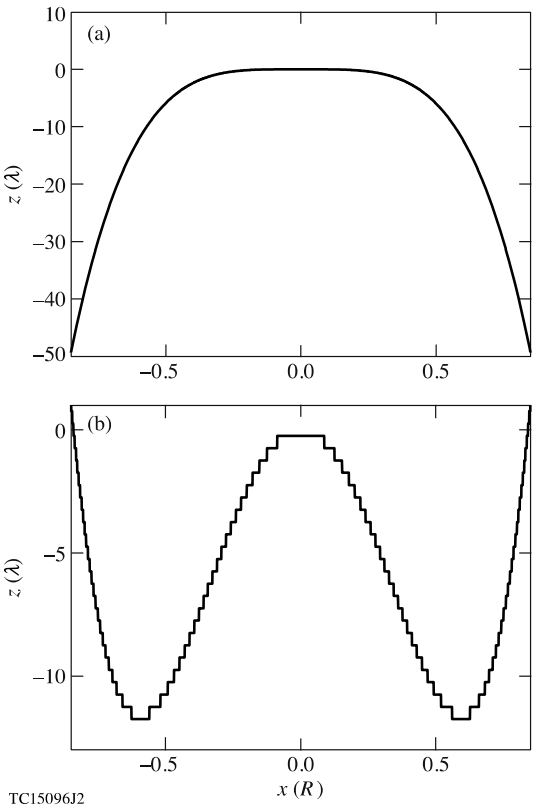

Figure 5. The spatial profiles (sag functions) of (a) the axiparabola after subtracting the parabolic profile and (b) the echelon used in the simulations.